



## Anti-Bacterial Activity of Plants Mediated Synthesized Titanium Oxide Nano Particles

Fatima, B. Salawu\*, Nma, N. Yahaya., Habib, A. Sadiq

Chemical Sciences Department, The Federal Polytechnic, Bida, Niger State

\*Email address: fatimabintu72@gmail.com

**Abstract** Microbial resistance represents a challenge for the scientific community to develop new bioactive compounds. Using nanoparticles for treatment of diseases caused by bacterial origin has mainly been considered. The impacts of antibacterial effect of plant extract mediated TiO<sub>2</sub> Nanoparticles (Nps) were investigated based on four bacteria *in vitro* and one bacteria *in vivo* analysis. In this experimental study, the presence of various photochemical like flavonoids, steroids, polyphenols, and terpenoids was investigated by following standard biochemical methods. The titanium oxide nanoparticles (TiO<sub>2</sub> NPs) synthesized was confirmed by their change of colour to brown and reddish brown due to the phenomenon of surface Plasmon resonance. The characterization studied was done by UV-vis spectroscopy, scanning electron microscopy (SEM), X-Ray diffraction (XRD) and Fourier Transmission infrared spectroscopy (FTIR). The green synthesized TiO<sub>2</sub> NPs excitation was confirmed using UV-Vis spectrophotometer at 270 and 290nm. SEM revealed that the synthesized TiO<sub>2</sub> NPs are spherical and crystalline in nature. The overall sizes are 40 and 50nm for *Blighia sapida* and *S. spinosa* respectively. FTIR spectroscopy analysis showed the presence of flavonoid, polyphenols and amide groups likely to be responsible for the green synthesis of titanium oxide nanoparticles using *B. sapida* and *S. spinosa* aqueous leaf extracts. The XRD pattern showed the characteristic Bragg peaks of (111), (200), (220) and (311) facets of the anatase titanium oxide nanoparticles and confirmed that these nanoparticles are crystalline and spherical in nature. It is evident from the zone of inhibition (19mm and 17mm) for *S. spinosa* and *B. sapida* respectively that TiO<sub>2</sub> nanoparticles possess potent bactericidal activity. In conclusion, this work proved the capability of using TiO<sub>2</sub> NPs to deliver a novel therapeutic route for antibacterial substances and also wound treatment in clinical practice.

**Keywords** *B. sapida*, *S. spinosa*, Titanium oxide, phytochemicals, antimicrobial activity, Wound healing activity; SEM; XRD; FTIR; UV-Vis spectroscopy

### Introduction

Nanobiotechnology, an emerging field of nanoscience, utilizes nanobased-systems for various biomedical applications. Nanoparticles usually referred to as particles with a size approximately smaller than 1  $\mu\text{m}$ , normally 1-100nm, (Christensen *et al.*, 2011). It exhibit completely new or improved properties based on specific characteristics such as size, high specific surface area, a high fraction of surface atoms and morphology. The nanoparticles possess unique physicochemical, optical, mechanical, diagnostic and biological properties which can be manipulated for desired applications (Christopher *et al.*, 2015); Din *et al.*, 2015). including catalytic activity, optical properties, electronic properties, antibacterial properties and magnetic properties (Zhao and Stevens, 1998; Crabtree *et al.*, 2003; The field of nanotechnology is one of the most active areas of research in modern material sciences. Recent nanotechnology holds a promise and a broad aspect towards wide applications of nanoparticles in a multiple way of emerging fields of science and technology.

As an important component in the development of nanotechnology, nanoparticles have been extensively explored for possible medical applications.

Antibiotics provide the main basis for the therapy of microbial (bacterial and fungal) infections and also the management of wounds.



Since the discovery of these antibiotics and their uses as chemotherapeutic agents there was a belief in the medical fraternity that this would lead to the eventual eradication of infectious diseases. However, over-use of antibiotics has become the major factor for the emergence and dissemination of multi-drug resistant strains of several groups of microorganisms (Chandra *et al.*, 2016). The worldwide emergence of microbial infections has become a major therapeutic problem. Multi-drug resistant strains of microbial infections are widely distributed in hospitals and are increasingly being isolated from community acquired infections (Weir *et al.*, 2012, Chang *et al.*, 2002). Nanoparticles are finding important applications in the field of medicine, (Dahl *et al.*, 2007). They provide solutions to technological and environmental challenges in the areas of solar energy conversion, catalyses, and water treatment (Damle *et al.*, 2016, Chung *et al.*, 2016). Nanomaterials particularly metallic nanoparticles have assumed a great deal of importance as they often display unique and considerably modified physical, chemical and biological properties as compared to their counterparts of a macro scale (Damle *et al.*, 2016). Recently, titanium dioxide nanopowder has received much interest. This is due to its use in various applications such as cosmetics, paper and medical devices coating and gas sensors (Wang *et al.* 2010). As far as the treatment of infectious diseases is concerned, resistance has developed due to injudicious and insensible use of antimicrobial agents (Das *et al.*, 2013). From the time of immemorial, for the cure of infections, the inorganic antimicrobials such as silver and copper have been in practice (Dehpour, 2009). Some of the new potential of nanoparticles are in the area of diagnostics and biomolecular detection of diseases as well as antimicrobials in therapeutics of infectious diseases (Jain *et al.*, 2009). Various chemical and physical methods are involving for the synthesis of nanoparticles (Din *et al.*, 2015). The chemical and physical synthesis of nanoparticles is expensive and often involves the use of toxic, hazardous chemicals which may pose environmental risks (Divya and Nithya, 2015). Biological methods have been put ahead to be advantageous over other synthetic methods as they are cost effective and do not involve the use of toxic chemicals, high pressure, energy and temperatures (Christensen *et al.*, 2011). The Nanoparticle are biosynthesized using various biosources such as bacteria, fungi, yeast, plant extract. Synthesis using bio-organisms is compatible with the green chemistry principles. The biosynthesis is eco-friendly as are the reducing agent employed and the capping agent of the reaction (Dubey *et al.*, 2009). Hence developing of reliable biosynthetic and environment friendly approach has added much importance because of its eco-friendly products, biocompatibility and economic viability in the long run and also to avoid adverse effects during their application especially in medical field. Among the biological alternatives, plants and plant extracts seem to be the best option. Plants are nature's "chemical factories". They are cost efficient and require little or no maintenance. A vast repertoire of secondary metabolites is found in all plants which possess redox capacity and can be exploited for biosynthesis of nanoparticles. As a wide range of metabolites are presented in the plant products/extracts, nanoparticles produced by plants are more stable and the rate of synthesis is faster in comparison to microorganisms. Thus, the advantages of using plant and plant-derived materials for biosynthesis of metal nanoparticles have instigated researchers to investigate mechanisms of metal ions uptake and bio reduction by plants, and to understand the possible mechanism of metal nanoparticle formation in and by the plants. Biosynthesis of nanoparticles is a bottom up approach where the main reaction occurring is reduction/oxidation. The plant phytochemicals reducing properties are usually responsible for the preparation of metal and metal oxide nanoparticles. Recently nanoparticle synthesis were achieved using plant extract such as azadirachta indica, camellia sinensis, Nyctanthes arbor-tristis, coriandrum, nelumbo nucifera, ocimum sanctum and several others which is compatible with the green chemistry principles. The main phytochemicals responsible for the synthesis of nanoparticles are terpenoids, flavones, ketones, aldehydes, amides (Dwivedi *et al.*, 2010). The present work is based on the plant extracts of *B. sapida* and *S. spinosa* plant extract. They are medicinal plant ever known. These species are frequently cited as being used in herbal medicines since the beginning of the first century AD (Wang *et al.* 2005).

## Materials and Methods

**Sample Collections:** Fresh leaves of *B. sapida* and *S. spinosa* plants were collected from the biological garden of Federal Polytechnic, Bida (Latitude 9°4'60" N, Longitude 6°1'0" E), Niger State, Nigeria in 2017. Healthy Albino rodents were purchased from Animal Breeding Unit of Biochemistry Department, Federal University of Technology, Minna, Niger State, Nigeria. The animals were kept in clean plastic cages and maintained under standard laboratory conditions. They were allowed unrestricted access to rat pellets and water. The study was carried out according to the Guide for the Care and the Use of Laboratory Animals of the Institute of Laboratory Animal Resources, Commission of Life Sciences, National Research Council, USA (ILAS, 1997).

**Preparation of the plant extract:** The leaves of *B. sapida* and *S. spinosa* collected were thoroughly washed and rinsed in distilled water, and then room dried for two weeks. After which hands were used to break them into fine pieces. Then 500 g of each plant was smashed into 1000 ml of sterile distilled water in a gas jar and boiled at 60°C



for 15mins and then filtered through Whatman No.1 filter paper. The percentage yield of the plant extracts are 16% and 15.5% for *B. sapida* and *S. spinosa* respectively. The aqueous extracts were stored at 40°C in an incubator for further experiments (Liu *et al.*, 2013).

**Phytochemical screening of plant extracts:** The extracts were subjected to tests for secondary metabolites such as tannins, flavonoids, steroids, glycosides, alkaloids, glycosides and saponins. The tests were carried out using standard methods of analysis (Trease and Evans, 2002). Analyses were done in triplicate.

**Synthesis of TiO<sub>2</sub> nanoparticles from the extracts:** To prepare an aqueous solution of 1.0M TiCl<sub>4</sub>, 5.0 ml of TiCl<sub>4</sub> was measured using a suction pipette, and mixed with 100 ml of distilled water in a 250 ml Erlenmeyer flask. The content was swirled properly. The mixture was then stored at 40°C before use. To a 100 ml portion of each of the leaf extracts of *B. sapida*, and *S. spinosa*, 10 ml of the 1.0 M TiCl<sub>4</sub> solution was added in drops on a water bath at a constant temperature of 70°C for a period of 4 hours with constant stirring at 200rpm. The suspension produced was centrifuged at 2000 rpm for 20mins and the supernatant liquid decanted. The residue was repeatedly washed with de-ionized water. Centrifugation, decantation and washing processes were repeated thrice to remove any impurity from the surface of the titanium oxide nanoparticles (Prakash *et al.*, 2013). The precipitate obtained was dried in an oven at a temperature of 40°C for 30mins (Kim *et al.*, 2013). The synthesized titanium dioxide nanoparticle samples were then subjected to characterization by UV- Vis, FTIR, XRD and SEM.

**Uv-vis spectrophotometry determination:** About 10 ml each of plant extracts, plant extracts mediated titanium oxide nanoparticles and commercial TiO<sub>2</sub> nanoparticles sample in colloidal solutions were separately placed in the cell holder of a UV- Vis spectrophotometer (model UV 1800 Shimadzu, Japan), in order to determine the absorption spectrum of the sample using the range between 200 to 800 nm. Colloidal solution was obtained by mixing warm distilled water with synthesized TiO<sub>2</sub> (Liu *et al.*, 2013).

**Fourier-transform infrared (FTIR) spectroscopy analysis:** The determination of the functional groups on the surface of the plant extract mediated titanium oxide nanoparticles was investigated by using a FTIR spectrophotometer ((Perkin Elmer Spectrum 2, Germany), and the spectra were scanned in the range of 4000 – 400cm<sup>-1</sup> at a resolution of 4cm<sup>-1</sup>. The samples were prepared by dispersing each of the biosynthesized titanium oxide NPs and commercial TiO<sub>2</sub> nanoparticles uniformly in a matrix of dry KBr, and then compressed to form an almost transparent disc. KBr was used as a standard analyte for the samples (Liu *et al.*, 2013).

**Scanning electron microscopy (SEM) of the nanoparticle:** In order to determine the surface morphology of the synthesized nanoparticle, SEM machine (HITACHI Model S-3000H Japan) was used. Thin films of the samples (biosynthesized titanium oxide NPs and commercial TiO<sub>2</sub> nanoparticles) were prepared on a carbon coated copper grid by just dropping a very small amount of each sample on the grid; the film on the SEM grid was allowed to dry and the images of nanoparticles taken (Chandra *et al.*, 2016).

**X ray diffraction (XRD) analysis of the nanoparticles:** X-ray diffraction measurements of the biosynthesized titanium oxide NPs and commercial TiO<sub>2</sub> nanoparticles were recorded on X - ray diffractometer (Philips Analytical). The phase variety, particle size and material identification of the NPs were identified. The samples were taken in lids and put under instrument for analysis (Liu *et al.*, 2013).

#### Evaluation of Antibacterial Activities

**In vitro** Antibacterial activity: The anti-bacterial action of the synthesized plant extract mediated titanium dioxide nanoparticle, plant extracts and commercial TiO<sub>2</sub> nanoparticles were determined by the well-diffusion technique. The action against four clinical pathogens (*Bacillus subtilis*, *Staphylococcus aureus*, *Escherichia coli*, *Salmonella typhi*) was carried out using 6 mm wells being cut on Mueller-Hinton agar swabbed with individual pathogenic bacteria according to the method of Catauro *et al.* (2003). Four wells were cut in each plate where 50 ml/mg, 75 ml/mg, and 100 ml/mg of colloidal solution of as-synthesized nanoparticles, plant extracts and commercial TiO<sub>2</sub> nanoparticle were added separately.

Each of the biosynthesized TiO<sub>2</sub> nanoparticle was dissolved in warm distilled water and allowed to form colloidal solution. One well was maintained as control by adding sterilized distilled water, while to another group, Ampicillin manufactured by Alcimpil FN. (Farcoral, Mexico) was added to serve as standard drug. The plates were incubated for 24-48hr and checked for the zone of inhibition using the method of (Prakash *et al.*, 2013).

The experiments were carried out in triplicate. The results (mean value, n=3) were recorded by measuring the zones of growth inhibition surrounding the disc.

**Determination of Minimum Inhibitory Concentration (MIC):** The minimum inhibitory concentration of the extracts of *B. sapida* and *S. spinosa*, mediated TiO<sub>2</sub> nanoparticle, commercial TiO<sub>2</sub> nanoparticle and plant extract were determined using tube dilution method with Mueller Hinton broth used as diluents. The lowest concentration of the sample showing inhibition for each organism when the samples were tested for sensitivity was serially diluted in the test tubes containing Mueller Hinton broth. The organisms were inoculated into each tube containing the broth



and the extracts. The inoculated tubes were then incubated at 37°C for 24 hours. At the end of which the tubes were examined for the presence or absence of growth using turbidity as a criterion, the lowest concentration on the series without visible sign of growth (turbidity) was considered to be the minimum inhibitory concentration (MIC).

### Results and Discussion

**UV visible analysis:** The UV-Vis spectroscopy was used to determine the formation and the stability of the synthesized titanium oxide nanoparticles in aqueous colloidal solution. It is also used to predict the initial phytoconstituents in plant material. The UV spectrum of the prepared biosynthesized TiO<sub>2</sub> nanoparticles, commercial titanium oxide Nps and plant extracts presented in Figure 1, 2 and 3 indicated that they all display maximum absorption in the vicinities of 400 - 800nm. The spectrum showed the formation of peak in the wavelength of 229nm for the *S. spinosa*, mediated NPs, a peak in the wavelength of 231nm for the *B. sapida* mediated counterpart, a peak of 430nm for commercial titanium oxide nanoparticles respectively. The absorptions are as follows: 3.475, 3.678 and 1.27nm for *S. spinosa*, mediated NPs, *B. sapida* mediated NPs and commercial titanium oxide nanoparticles respectively (Kim *et al.*, 2013). The UV-Vis spectra of plant extracts of *S. spinosa*, *s mediated* TiO<sub>2</sub> Nps and plant extracts of *B. sapida mediated* TiO<sub>2</sub> Nps have high absorbance intensity compared to commercial titanium oxide nanoparticles. This is because, various metabolites from plant extract introduced to solution make the plasmon band broad and they may be read in the spectrophotometric with surface plasmon resonance (SPR) was responsible for exhibiting the absorption of UV-Vis radiation (Kim *et al.*, 2013), These wave lengths arise due to the surface Plasmon resonance of the particle (Joshin *et al.*, 2008). The magnitude of peak, wavelength and spectral bandwidth associated with nanoparticles are dependent on size, shape and material composition (Prakash *et al.*, 2013, Kim *et al.*, 2013). These changes in their properties increases their interacting faces thereby considered as enhancement in terms of absorption of wave length spectrum in the UV-Vis region. Commercial TiO<sub>2</sub> Nps had the least absorption. As indicated in Figure 4 and 5. This was similar to the trend obtained by Salam *et al.*, (2012) in the work done on synthesised Citrus paradisi peel extract mediated titanium dioxide nanoparticles. and biological synthesis of TiO<sub>2</sub> nanoparticles using extracts of *Ananas comosus* (Anwar *et al.*, 2010, Wilkinson *et al.*, 2011).

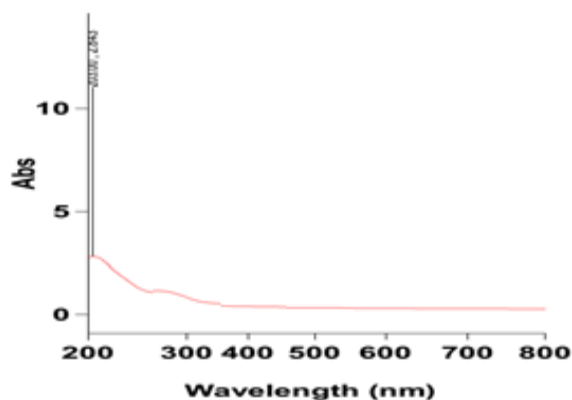


Figure 1: UV-Vis spectra of titanium oxide nanoparticles synthesized by *B. sapida*

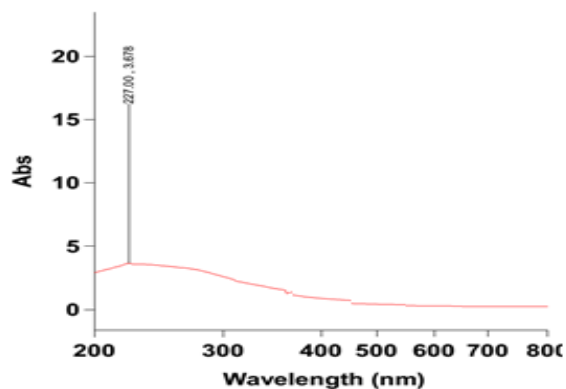


Figure 2: UV-Vis spectra of titanium oxide nanoparticles synthesized by *S. spinosa*

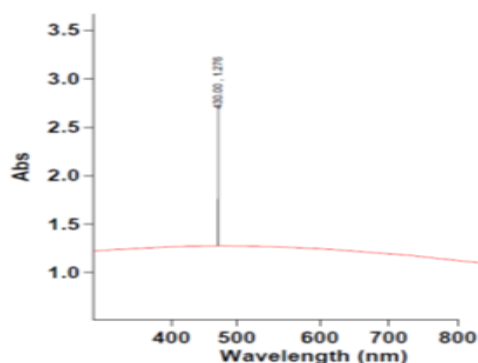


Figure 3: U-visible spectrum of commercial titanium oxide of nano particle

**Fourier Transform Infrared Spectroscopic Study:** FTIR analysis was used to find out the reduction of TiO<sub>2</sub> nanoparticles by biomacromolecules present in the plant extract. These biomacromolecules are responsible for the reduction and stabilization of TiO<sub>2</sub> nanoparticles. Figure 4, 5 and 6 shows the FT-IR spectrum of *B. sapida* mediated TiO<sub>2</sub> NPs, *S. spinosa*, mediated TiO<sub>2</sub> NPs and that for commercial TiO<sub>2</sub> NPs, respectively.

**B. sapida mediated TiO<sub>2</sub> NPs:** The characteristic absorption bands were exhibited at 2920cm<sup>-1</sup> (for C-H stretching) and at 1602.8cm<sup>-1</sup> for carbonyl group (C=O), and at 3678.9cm<sup>-1</sup> for Hydroxyl(-OH) group; Amine at 2920cm<sup>-1</sup> and 1513cm<sup>-1</sup> for (C=C) stretching vibration.

**S. spinosa, mediated TiO<sub>2</sub> NPs:** mediated TiO<sub>2</sub> NPs showed characteristic absorption bands at 3220cm<sup>-1</sup> for hydroxyl (-OH) group, 1617cm<sup>-1</sup> (for (C=O) stretching), absorption at 1282cm<sup>-1</sup> (for C-N stretching) and at 1438cm<sup>-1</sup> for alkyl group.

**Commercial TiO<sub>2</sub> NPs:** Figure 6 indicated commercial TiO<sub>2</sub> NPs characteristic absorption bands were exhibited at 3712 - 3768cm<sup>-1</sup> for hydroxyl (-OH) group and at 1654cm<sup>-1</sup> for carbonyl group (C=O). From the FTIR results (Figure 10) there is presence of hydroxyl groups of phenols, carbonyl group (C=O), alkyl group. Bali *et al.* (2006) reported same with also amide group, these form layers on the nanoparticles and acting as a capping agent to prevent agglomeration and providing stability in the medium in the work on extract of *N. tabacum* Leaves mediated silver Nps. The functional groups in the FTIR results support the presence of phenolic compounds (flavonoids) in the extracts as evidenced by phytochemical analysis. Raymond *et al.* (2009) reported that the band at 1742cm<sup>-1</sup> is characteristic of stretching vibrations of the carbonyl functional group in ketones, aldehydes and carboxylic acids in the study on *Micrococca mercurialis*

**Table 1:** FTIR absorption frequencies of plant leaf extract mediated TiO<sub>2</sub> nanoparticles. Assignments of FTIR peaks of BS and SS

Note:, BS= *B. sapida* and SS = *S. spinosa*

Wavenumber (cm <sup>-1</sup> )	Assignments
<b>AS</b>	
3257.7	O-H stretching vibration
2926.0	Asymmetric C-H stretching
2113.4	overtone and/or combinational bands
1606.5	C=C aromatic
1438.8	C-H in-plane deformation
1375.4	C-H symmetric deformation
1282.2	C-O stretch
1073.5	C-O asymmetric stretch
<b>HT</b>	
3220.4	O-H stretching mode
2113.4	overtone and/or combinational bands
1617.7	C=C aromatic
1524.5	C=C aromatic
1438.8	C-H in-plane deformation
1282.2	C-O asymmetric stretch
1110.7	C-O stretch



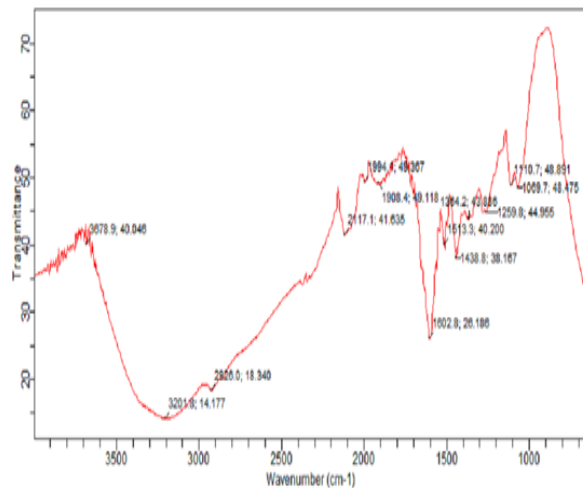


Figure 4: FTIR spectra from solid powder titanium oxide nanoparticles by *B. sapida* extract

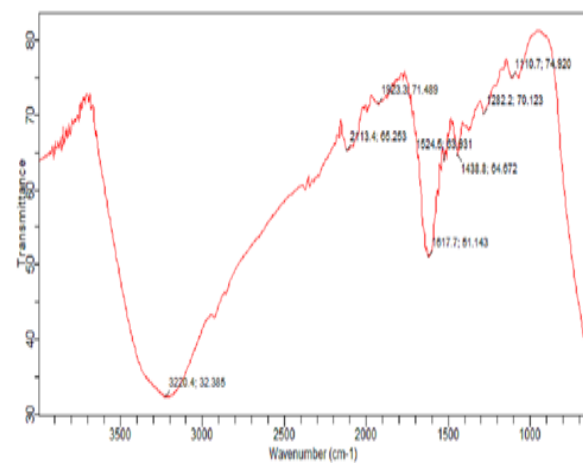


Figure 5: FTIR spectra from titanium oxide nanoparticles by *S. spinosa*

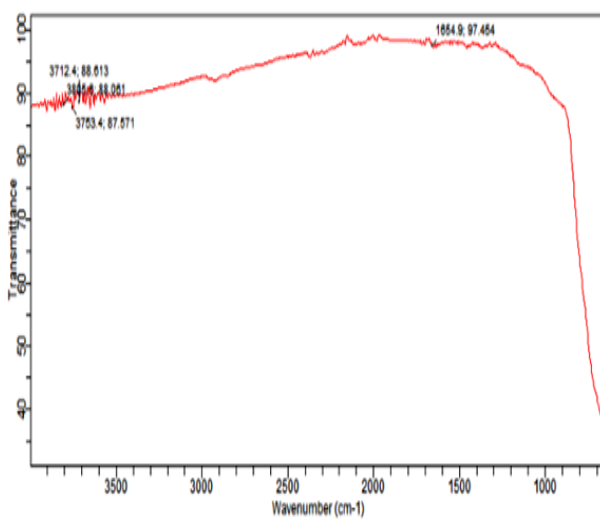


Figure 6: FTIR spectra from by Fine commercial powdered titanium oxide nanoparticles

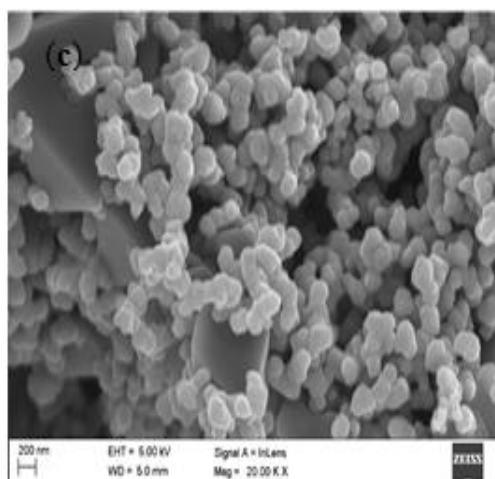


Figure 7: Scanning electron microscopy image of the biosynthesis of TiO<sub>2</sub> nanoparticle by *B. Sapida*

Based on these FTIR studies, it can be suggested that the bio-molecules present in the plant extracts of *B. sapida* and *S. spinosa* play dual role in formation and stabilization to TiO<sub>2</sub> nanoparticles

Scanning Electron Microscopic analysis: Fig.7, 8 and 9 shows the SEM images of biosynthesised TiO<sub>2</sub> nanoparticles obtained using leaf extracts of *B. sapida*, *S. spinosa* and commercial TiO<sub>2</sub> nanoparticles respectively. The image describes the surface morphology of the TiO<sub>2</sub> nanoparticles. The green synthesized TiO<sub>2</sub> nanoparticles showed monodispersity without aggregation when compared to that of the commercial TiO<sub>2</sub> nanoparticles. This is due to the capping of TiO<sub>2</sub> nanoparticles with the compounds present in the leaf extract. The particles were found to be spherical with distinct edges and without aggregation. Previous reports showed that phytochemical compound in nanoparticles are disaggregated and are stable with good dispersibility. Edison and Sethuraman (2013) supports the present findings in the work on The *Origanum vulgare* aqueous leaf extract. It could therefore be speculated that the phytochemicals in these leaf extracts coats the surface of the TiO<sub>2</sub> nanoparticles thus preventing their aggregation. The SEM images showed average sizes of 50nm, 40 nm and 72nm for biosynthesised TiO<sub>2</sub> nanoparticles obtained using leaf extracts of *B. sapida*, *S. spinosa* and commercial TiO<sub>2</sub> nanoparticles respectively. The images showed that the samples are spherical in shape. Titanium dioxide nanoparticle of approximate diameter 50-60nm have been previously reported (Raymond *et al.*, 2009). The TiO<sub>2</sub>-NPs, of these sizes showed that nanoparticles produced by this method were primarily crystalline (Wang *et al.*, 2005; Ismagijov *et al.*, 2009).

The XRD pattern of TiO<sub>2</sub> nanoparticles obtained using flower extract of *B. sapida* and *S. spinosa* are shown in Fig. (10, 11 and 12) A sharp diffraction peak was observed with slight broadening peak for green synthesized TiO<sub>2</sub> nanoparticles. The lattice parameters obtained were close and consistent with standard data for TiO<sub>2</sub> (JCPDS 21-1272) (Prakash *et al.*, 2013). We have calculated the average crystallite size of TiO<sub>2</sub> nanoparticles synthesized by green route using the Scherrer's formula ( $d = 0.89 \lambda / \beta \cos\theta$ ).

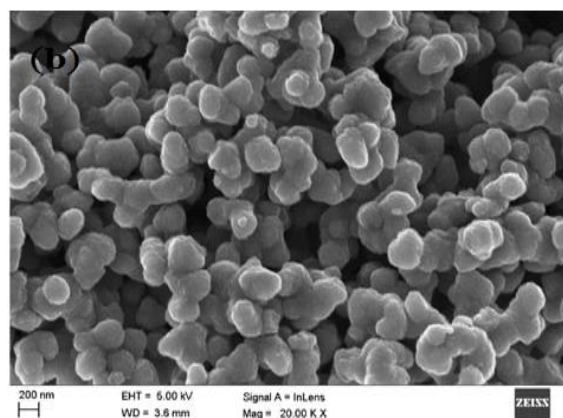


Figure 8: Scanning electron microscopy image of the biosynthesis of TiO<sub>2</sub> nanoparticle by *S. spinosa*



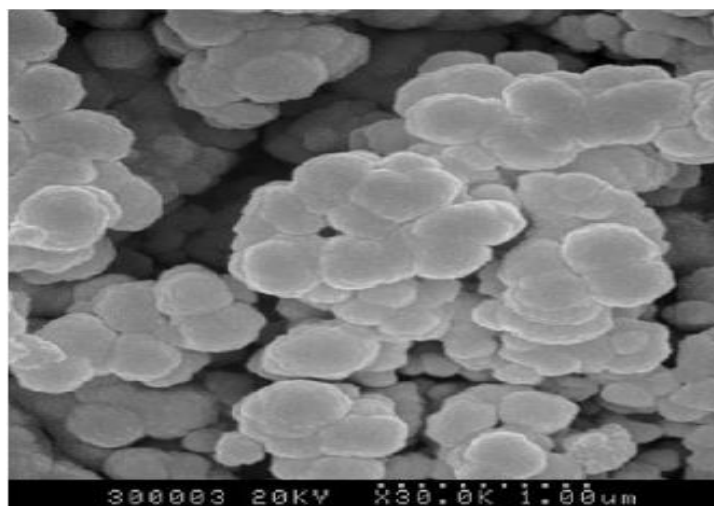


Figure 9: Scanning electron microscopy image of the Commercial  $\text{TiO}_2$  nanoparticle

The calculated crystallite was found to be 58nm, 43nm, 45nm and 42 nm respectively. nm for green synthesized  $\text{TiO}_2$  nanoparticles. The results of XRD analysis confirm the presence of  $\text{TiO}_2$  nanoparticles in the green synthesized sample. Previous reports have also used XRD as an evidence for the confirmation of  $\text{TiO}_2$  nanoparticles (Liu *et al.*, 2013). The XRD peaks of green synthesized  $\text{TiO}_2$  nanoparticles obtained using the above extract. Ahmad and Seema (2012) have reported the correlation between XRD peak broadening and the size reduction during green synthesis protocol. Thus, the broadening of XRD peak of green synthesized  $\text{TiO}_2$  nanoparticles observed in our study confirms the size reduction. Earlier reports on XRD data of nanoparticles have documented an inverse relation between peak intensity and surface functionalization of nanoparticles (Daizy, P. 2009). Surface coating of the nanoparticles with functional groups (i.e, surface functionalization) results in an internal strain in the particles consequently decreasing the signal: noise ratio. As a result, the intensity of the XRD peak decreases (Daizy, P. 2009). Therefore, we suggest that the phytochemicals present in the extracts would have coated the surface of the  $\text{TiO}_2$  nanoparticles, resulting in decreased intensity in XRD peak. This phytochemical coating may enhance the stability and the dispersibility of the nanoparticles, which in turn may enhance their bioavailability, making them suitable for biological applications. The XRD profile reveals that the green synthesis protocol that we developed using *B. sapida* and *S. spinosa* is valid for the production of bio functionalized and bio-stabilized titanium nanoparticles with potential biomedical activities.

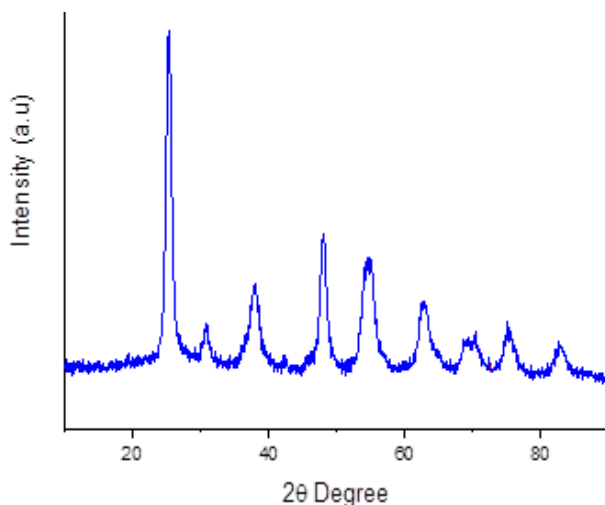


Figure 10: XRD images of biosynthesized  $\text{TiO}_2$  NPS by *B. sapida* extract



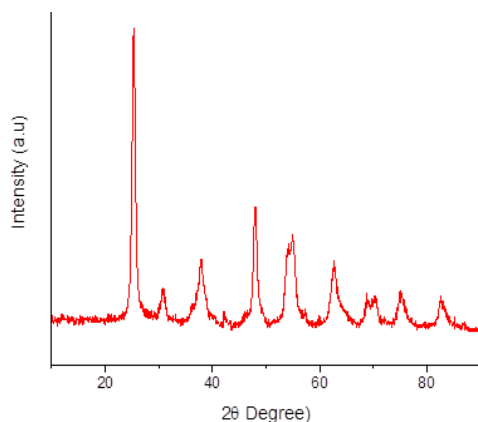


Figure 11: XRD images of biosynthesized  $\text{TiO}_2$  NPS by *S. spinosa* extract

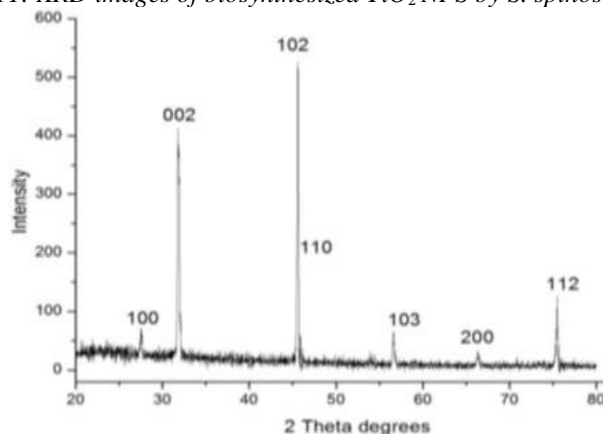


Figure 12: XRD of commercial  $\text{TiO}_2$  nano particles

**Antimicrobial activities of Nanoformulated  $\text{TiO}_2$  NPs:** The antimicrobial activity of the extracts of *B. sapida* and *S. spinosa* mediated  $\text{TiO}_2$  nanoparticle was compared with that of commercial  $\text{TiO}_2$  nanoparticle and the extracts of *B. sapida* and *S. spinosa* against four microbial pathogens by agar well diffusion method successfully. The antibacterial activity results revealed that the biosynthesised  $\text{TiO}_2$  nanoparticles acted as excellent antibacterial agents against both Gram-positive and Gram-negative bacteria when compared with commercial  $\text{TiO}_2$  nanoparticles and plant extracts of *B. sapida* and *S. spinosa*. Tables 2, 3 and 4, and Figures 17,18 and 19 show the values and zones of inhibitions produced by the green synthesized  $\text{TiO}_2$  nanoparticles, commercial  $\text{TiO}_2$  nanoparticles and the plant extracts of *B. sapida* and *S. spinosa* against both Gram-positive and Gram-negative bacterial strains. *B. sapida* mediated  $\text{TiO}_2$  nanoparticles exhibited maximum (15mm) bacterial growth inhibition against *B. subtilis* while *S. spinosa* mediated  $\text{TiO}_2$  nanoparticles exhibited maximum (14mm) bacterial growth inhibition against *B. subtilis*, in the form of zone-of-inhibition studies, where diffusion of nanoparticles on nutrient agar plates inhibits growth. In contrast, the commercial  $\text{TiO}_2$  nanoparticles showed zones of inhibition of (11mm) against *B. subtilis* and plant extracts showed (10.5mm). In the case of *E. coli* maximum growth, inhibition zones were found to be as follows: 17, 12, 8 and 7 mm for *B. sapida* and *S. spinosa* leaf extract mediated  $\text{TiO}_2$  nanoparticles, commercial nanoparticles  $\text{TiO}_2$  and plant extracts respectively. Similar patterns were observed in the case of *S. aureus*, where the maximum zone of inhibition was exhibited by *B. sapida*  $\text{TiO}_2$  nanoparticles followed by *S. spinosa*  $\text{TiO}_2$  nanoparticles and commercial nanoparticles  $\text{TiO}_2$ . Plant extracts of *B. sapida* and *S. spinosa* showed zones of inhibition of 10.5 mm against *B. subtilis*.

Nanoparticles tend to adsorb on the bacterial cell and undergo dehydrogenation due to respiration process which occurs at the cell membrane of bacteria. Biosynthesised Titanium oxide nanoparticles and commercial nanoparticles  $\text{TiO}_2$  have shown antibacterial activities more than the extract of *B. sapida* and *S. spinosa* alone, because they have very large surface area to volume ratio, having high surface area to volume ratio in nanocrystals can lead to unexpected properties, increasing their reactivity tremendously as they have a greater number of reaction sites and can provide better contact with microorganisms.



**Table 2:** Antibacterial activity of nanoformulated Titanium Oxide NPs. Data are express as Mean  $\pm$ SEM of triplicate determination. Values followed by different superscript alphabet were significantly different ( $p < 0.05$ )

Plant extract/ concentration (mg/mL)	Test organisms/zone of inhibition (mm)			
	<i>Staphylococcus aureus</i>	<i>Bacillus subtilis</i>	<i>Escherichia coli</i>	<i>Salmonella typhi</i>
<i>B. sapida</i>				
100	0	0	18.65 $\pm$ 0.32 <sup>c</sup>	16.45 $\pm$ 0.33 <sup>b</sup>
50	0	0	16.05 $\pm$ 0.94 <sup>b</sup>	14.65 $\pm$ 0.92 <sup>ab</sup>
25	0	0	14.67 $\pm$ 0.93 <sup>ab</sup>	12.06 $\pm$ 0.14 <sup>a</sup>
12.5	0	0	12.56 $\pm$ 0.23 <sup>a</sup>	11.54 $\pm$ 0.52 <sup>a</sup>
<i>S. spinosa</i>				
100	18.05 $\pm$ 0.26 <sup>c</sup>	0	0	16.54 $\pm$ 0.55 <sup>b</sup>
50	16.67 $\pm$ 0.26 <sup>b</sup>	0	0	14.67 $\pm$ 0.17 <sup>ab</sup>
25	14.76 $\pm$ 0.50 <sup>ab</sup>	0	0	13.83 $\pm$ 0.43 <sup>ab</sup>
12.5	12.04 $\pm$ 0.27 <sup>a</sup>	0	0	11.43 $\pm$ 0.55 <sup>a</sup>

Data are express as Mean  $\pm$ SEM of triplicate determination. Values followed by different superscript alphabet were significantly different ( $p < 0.05$ )

**Table 3:** MIC of nanoformulated Titanium Oxide NPs against bacteria isolates

Plant extract/ concentration (mg/ml)	<i>Staphylococcus aureus</i>	<i>Bacillus subtilis</i>	<i>Escherichia coli</i>	<i>Salmonella typhi</i>
<i>B. sapida</i>				
12.5	-	-	-	-
6.25	-	+	-	-
3.125	+	+	+	-
1.5	+	+	+	-
<i>S. spinosa</i>				
12.5	-	-	-	-
6.25	-	-	-	-
3.125	-	-	+	+
1.5	-	-	+	+

Surfaces of nanoparticles affect/interact directly with the bacterial outer membrane, causing the membrane to rupture and killing bacteria due to its extremely small size. The as-synthesized TiO<sub>2</sub> nanoparticle had more effectiveness and efficacy against microbial activity than does the commercial TiO<sub>2</sub> nanoparticle, because of the capping agent (phytochemicals) from the plant extract in the as-synthesized TiO<sub>2</sub> nanoparticle. These are saponins, tannins, flavonion, alkaloids, phenolic compounds, terpenoids, etc. These are plant metabolites known for antimicrobial activity (Dehpour *et al.*, 2009). The antimicrobial activity in terms of inhibition zone significantly varied with test microbes and the type of the extracts. Although the as-synthesized TiO<sub>2</sub> nanoparticles and commercial TiO<sub>2</sub> nanoparticle in the present study were observed to have strong antimicrobial potential, plant extracts of *B. sapida* and *S. spinosa* were found to be less active against the tested bacterial. Effectiveness of plant extracts depends on their active compound, for example, some of them like flavonoid, tannins and terpenoids are highly soluble in water but have low absorption capacity because they are unable to cross the lipid membrane of the cells. They have excessively high molecular size or are poorly absorbed resulting in loss of bioavailability and efficacy. Some have low solubility, poor permeability and instability in biological environment. This limitation can be overcome by encapsulating or attaching them with material known as nanomaterials. When the result was compared with the antibiotics like Ampillicin, Tobramycin and Erythromycin, nanoparticles were found to be more potent than antibiotics.



## Conclusion

The present study reports the biosynthesis of TiO<sub>2</sub>NPs, by *B. sapida* and *S. spinosa* leaf extract, confirmed by XRD, UV-vis spectroscopy and FTIR analyses. Antimicrobial activities of the biosynthesised TiO<sub>2</sub>NPs were evaluated towards pathogenic bacteria. The Bio-synthesized TiO<sub>2</sub> nanoparticles exhibited higher antibacterial activity against pathogenic bacteria compared to commercial TiO<sub>2</sub> and the plant extracts.

The results of this study introduced remarkable *in vitro* TiO<sub>2</sub> NPs accelerating effects on the treatment of bacterial infections with no obvious side effects in the rats. To our knowledge, this therapy has not been investigated before. It has proved efficient and promising in managing infections caused by bacteria and it could be used as an alternative to conventional antibiotic therapy. Based on these results, it is concluded that the leaf extracts stabilized TiO<sub>2</sub> nanoparticles and this made it to have higher potential biomedical applications when compared to commercial TiO<sub>2</sub> nanoparticles.

## References

- [1]. Ahmed, N and Seema, S. (2012) Green synthesis of silver nanoparticles using extracts Anansacomosus. Green and sustainable Chemistry 2, 141 - 147
- [2]. Anwar, N.S., Kassim, A., Lim, H.N., Zakarya, S.A and Huang, N.M. (2010). Synthesis of Titanium Dioxide Nanoparticles via Sucrose Ester Micelle-Mediated Hydrothermal Processing Route. SainsMalaysiana, 39 (2): 261-265.
- [3]. Bali, R., Razak, N., Lumb, A. and Harris, A.T. (2006). The synthesis of metallic nanoparticles inside live plants. Laboratory for Sustainable Technology, School of Chemical and Biomolecular Engineering.
- [4]. Catauro, M., Raucci, M.G., De Gaetano, F.D and Marotta. A. (2004). "Antibacterial and bioactive silver-containing Na<sub>2</sub>O.CaO.2SiO<sub>2</sub> glass prepared by sol-gel method. Journal of Material Science: Material in Medicine. 15: 831-837.
- [5]. Chandra, S.E., Krishna R., Rao, K. and Kumar, S.P. (2016). A green approach to synthesize controllable silver nanostructures from Limonia acidissima for inactivation of pathogenic bacteria Cogent Chemistry.
- [6]. Chang, C., Yang, M., Wen, H. and Chen, J. (2002) Estimation of total flavonoid content in Propolis by two complementary colorimetric methods. Journal of Food Drug Analysis. 10: 178–182.
- [7]. Christensen, L., Vivekanandhan, S., Misra, M. and Mohanty, A.K. (2011). Biosynthesis of silver nanoparticles using *Murraya koenigii* (curry leaf): an investigation on the effect of broth concentration in reduction mechanism and particle size. Advanced Material Letters. 2: 429–434.
- [8]. Christopher, J., Banerjee, S. and Panneerselvam, E. (2015). Optimization of parameters for biosynthesis of silver nanoparticles using leaf extract of *Aegle marmelos*. Brazillian Archives of Biology Technology. 58: 702–710
- [9]. Chung, I.M., Park, L., Seung-Hyun, K., Thiruvengadam, M. and Rajakumar, G. (2016). Plant mediated synthesis of silver nanoparticles: their characteristics properties and therapeutic applications. Nanoscale Research Letter, 11: 1–14.
- [10]. Chung, I.M., Park, Seung-Hyun, K., Thiruvengadam, and Rajakumar, G. (2016). Plant mediated synthesis of silver nanoparticles: their characteristics properties and therapeutic applications. Nanoscale Research letters. 11: 1–14.
- [11]. Crabtree, J.H., Burchette, R. J., Siddiqi, R.A., Huen, I.T., Hadnott, L.L. and Fishman, A. (2003) "The efficacy of silver-ion implanted catheters in reducing peritoneal dialysis-related infections. Peritoneal Dialysis International. 23: 368-374.
- [12]. Dahl, J.A., Maddux, B. and Hutchison, J.E. (2007). Toward greener nanosynthesis Chem. Rev. 107: 2228–2269.
- [13]. Daizy P. (2009). Biosynthesis of Au, Ag and Au–Ag nanoparticles using edible mushroom extract, Spectrochimica Acta Part A: Molecular and Biomolecular Spectroscopy, 374–381.
- [14]. Damle, P., Hegde, D., Nayak, S. and Vaman, C.R. (2016). Green synthesis of silver nanoparticles from Santalum album tender leaf extract and evaluation of its antioxidant capacity. Indian Journal of Advances in Chemical Science SI. 253–257.
- [15]. Das, J., Das, M.P. and Velusamy, P. (2013). Sesbania grandiflora leaf extract mediated green synthesis of antibacterial silver nanoparticles against selected human pathogens. Spectrochimica. Acta part A: Molecular and Biomolecular Spectroscopy. 104: 265–270.
- [16]. Das, J., Das, M.P. and Velusamy, P. (2013). Sesbania grandiflora leaf extract mediated green synthesis of antibacterial silver nanoparticles against selected human pathogens. Spectrochimica Acta Part A: Molecular and Biomolecular Spectroscopy. 104: 265–270.



- [17]. Dehpour, A., Ebrahimzadeh, M., Nabavi, S. and Nabavi, S.M. (2009). Antioxidant activity of methanol extract of *Ferula assafoetida* and its essential oil composition. *Grasas Aceites.*, 60: 405–412.
- [18]. Dehpour, A., Ebrahimzadeh, M., Nabavi, S. and Nabavi, S.M. (2009). Antioxidant activity of methanol extract of *Ferula assafoetida* and its essential oil composition. *Grasas Aceites.*, 60: 405–412
- [19]. Din, L., Mie, R., Samsudin, M., Ahmad, A. and Ibrahim, N. (2015). Biomimetic synthesis of silver nanoparticles using the lichen *Ramalina dumeticola* and the antibacterial activity. *Malaysian journal of analytical sciences* 19: 369–376.
- [20]. Divya, P. and Nithya, T. (2015). Silver nanoparticles eco-friendly synthesis by ornamental flower extracts and evaluation of their antimicrobial activity. *International journal of Research in pharmaceutical and Nano Sciences*, 4: 250–259.
- [21]. Dubey, M., Bhadauria S. and Kushwaha B. (2009) Green synthesis of nanosilver particles from extract of *Eucalyptus hybrida* (safeda) leaf. *Digital Journal of Nanomaterials and Biostructures*. 4: 537–543.
- [22]. Dwivedi, A.D. and Gopal, K. (2010). Biosynthesis of silver and gold nanoparticles using *Chenopodium album* leaf extract. *Colloids Surfaces, A*. 369: 27–33.
- [23]. Edison, T. and Sethuraman, M. (2013). Biogenic robust synthesis of silver nanoparticles using *Punica granatum* peel and its application as a green catalyst for the reduction of an anthropogenic pollutant 4-nitrophenol. *Spectrochimica Acta Part A: Molecular and Biomolecular Spectroscopy*, 104: 262–264.
- [24]. ILAS, (1997). Institute of Laboratory Animal Resources, Commission of Life Sciences. National Research Council.
- [25]. Ismagilov, Z. R., Tsykoza, L.T., Shikina, N.V., Zarytova, V.F., Zinoviev, V.V and Zagrebnyi, S.N. (2009). Synthesis and stabilization of nano-sized titanium dioxide. *Russ. Chemistry Research*, 78 (9) 1-13. 43.
- [26]. Jani, D., Daima, H. K., Kachwaha, S and Kothari, S. L. (2009). Synthesis of plant mediated silver nano particles using papaya fruit extract and evaluation of their antimicrobial activities. *Digital journal of nano material biosynthesis*, 4: 557-563.
- [27]. Joshi, M., Bhattacharyya, A. and Ali, S. W. (2008). Characterization techniques for nanotechnology applications in textiles. *Indian journal of fibre & textile research*. 33: 304–317.
- [28]. Kim, D.H., Ryu, H.W., Moon, J.H and Kim, J. (2013). Effect of ultrasonic treatment and temperature on nanocrystalline TiO<sub>2</sub>. *Journal of Power Sources*, 163 (1): 196-200.
- [29]. Liu, C.M., Guo, L., Xu, H.B., Wu, Z.Y and Weber, J. (2013) Seed mediated growth and properties of copper nanoparticles, nanoparticle 1D arrays and nanorods. *Microelectronic Engineering*. 66: 107-114.
- [30]. Prakash, P., Gnanaprakasam, P., Emmanuel, R., Arokiyaraj, S. and Saravanan, M. (2013). Green synthesis of silver nanoparticles from leaf extract of *Mimusops elengi*, Linn. for enhanced antibacterial activity against multi drug resistant clinical isolates. *Colloids Surfaces. B: Biointerfaces* 1:255–9.
- [31]. Raymond, F.H.J., Nianqiang, W., Dale, P., Mary, B., Michael, W and Andrij, H. (2009). Particle length-dependent titanium dioxide nanomaterials toxicity and bioactivity. *Part. Fibre Toxicology.*, 6 (12): 1-11.
- [32]. Salam, H.A., Rajiv, P., Kamaraj, M., Jagadeeswaran, P., Gunalan, S and Sivaraj, R. (2012). Plants: green route for nanoparticle synthesis. *International Research Journal of Biological Science*. 115: 2547–2564.
- [33]. Trease, G.E and Evans, W.C. (2002). *Phytochemical Screening and In vitro Bioactivity of Cnidioscolus*. WB Saunders, Edinburgh, 15th Ed, 211-242.
- [34]. Wang, J., B., Mao, J., Gole, L and Burda, C. (2010). Visiblelight- driven reversible and switchable hydrophobic to hydrophilic nitrogen doped titania surfaces: correlation with photocatalysis. *Nanoscale*. 2: 2257-2261.
- [35]. Wang, W., Lenggoro, I.L., Terashi, Y., Kim, T.O and Okuyama, K. (2005). One-step synthesis of titanium oxide nanoparticles by spray pyrolysis of organic precursors. *Material Science Engineering*, 123 (3): 194-202.
- [36]. Weir A., Westerhoff P., Fabricius L., Hristovski K. and Von Goetz N. (2012). Titanium dioxide nanoparticles in food and personal care products. *Environmental Science and Technology*. 46(4):2242-50.
- [37]. Wilkinson, L.J., White, R.J., Chipman, J.K. (2011). Silver and nanoparticles of silver in wound dressings: a review of efficacy and safety. *Journal of Wound Care*. 20: 543–9.
- [38]. Zhao, G and Stevens, S. E. (1998). “Multiple Parameters for the Comprehensive Evaluation of the Susceptibility of *Escherichia coli* to the Silver Ion, *Bio Metals*. 11: 27-32.

